

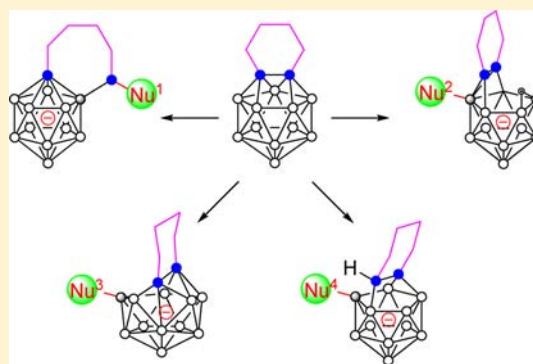
Reaction of 13-Vertex Carborane μ -1,2-(CH₂)₄-1,2-C₂B₁₁H₁₁ with Nucleophiles: Linkage Effect on Product Formation

Jian Zhang and Zuwei Xie*

Department of Chemistry and State Key Laboratory of Synthetic Chemistry, The Chinese University of Hong Kong, Shatin, New Territories, Hong Kong, China

Supporting Information

ABSTRACT: The length of C,C'-linkage has a great influence on the reactivity of 13-vertex carboranes. Reaction of 1,2-(CH₂)₄-1,2-C₂B₁₁H₁₁ (**1a**) with Et₂NH gave a 1:1 adduct *nido*-7-NEt₂H- μ -1,3-(CH₂)₄-1,3-C₂B₁₁H₁₁ (**2**). Compound **1a** reacted with Me₂NLi or Et₂NLi to afford *nido*-[9-Nu- μ -7,8,10-(CH₂)₄CCH-B₁₁H₁₀]⁻ (Nu = NMe₂, [**3**]⁻; Nu = NEt₂, [**4**]⁻). Complex [**4**]⁻ was also obtained by deprotonation of **2**. Treatment of **1a** with MeOH/base generated *nido*-[3-OMe- μ -1,2-(CH₂)₄-1,2-C₂B₁₁H₁₁]⁻ ([**5**]⁻) at room temperature, which was converted to *nido*-[μ -7,8-(CH₂)₄CHB(OMe)₂-7-CB₁₀H₁₁]⁻ ([**6**]⁻) upon heating in the presence of Et₃N. Complex [**6**]⁻ was oxidized by H₂O₂ to the corresponding alcohol [μ -7,8-(CH₂)₄CHOH-7-CB₁₀H₁₁]⁻ ([**7**]⁻) or hydrolyzed to the boronic acid [μ -7,8-(CH₂)₄CHB(OH)₂-7-CB₁₀H₁₁]⁻ ([**8**]⁻). Reaction of **1a** with (4-MeC₆H₄)SNa produced a CB₁₁⁻ anion *closo*-[μ -1,2-(CH₂)₄CHS(4-MeC₆H₄)-1-CB₁₁H₁₀]⁻ ([**9**]⁻). The above complexes were fully characterized by ¹H, ¹³C, and ¹¹B NMR spectroscopic data and elemental analyses. Molecular structures of **1**–[**7**]⁻ and [**9**]⁻ were further confirmed by single-crystal X-ray analyses.



INTRODUCTION

Studies of supercarboranes (carboranes with more than 12 vertices) remain a young research area,¹ particularly in comparison to the rich literature of icosahedral carboranes.² Only in the recent decade, several 13- and 14-vertex carboranes have been prepared^{3–8} using carbon-atoms-adjacent carborane anions as starting materials.⁹ These supraicosahedral molecules share some chemical properties with those of icosahedral species; and on the other hand, they have their own unique characteristics.

The electrophilic substitution reaction of 13-vertex carborane μ -1,2-(CH₂)₃-1,2-C₂B₁₁H₁₁ (**1b**) gives 8,9,10,11,12,13-X₆- μ -1,2-(CH₂)₃-1,2-C₂B₁₁H₅ (X = Me, Br, I),⁵ in which the six BH vertices that are farthest from the cage carbons are substituted, a phenomenon similarly observed in 12-vertex analogues.¹⁰ Compound **1b** can undergo single-electron reduction to generate a stable carborane radical anion with [2n + 3] framework electrons,¹¹ which is very uncommon for a 12-vertex one.¹² In the presence of an excess amount of group 1 metals, both 13- and 14-vertex carboranes can be readily reduced to the corresponding *nido*-carborane dianions,^{4–8} whereas 12-vertex carboranes can even undergo 4e⁻ reduction to yield *arachno*-carborane tetraanions.^{9a,c,d,13} Under strong basic conditions, α -deprotonation of the methylene chain proceeds to produce the monoanion [1,2-CH(CH₂)₂-1,2-C₂B₁₁H₁₁]⁻ with *exo* C=C π bonding.¹⁴ Moreover, **1b** can react with various nucleophiles to give cage boron and/or carbon extrusion products *closo*-CB₁₁⁻, *nido*-CB₁₀⁻, *closo*-CB₁₀⁻

anions, or *closo*-C₂B₁₀, depending on the nature of nucleophiles.^{15–17} It is noted that the extruded cage C becomes one of the carbon-chain atoms in the above reactions, leading to the formation of CB₁₁⁻ anions with an *exo* six-membered ring. We wondered whether the length of the carbon-chain linkage plays a role in these cage transformation processes. With this in mind, we extended our research to a 13-vertex carborane with four methylene linkage μ -1,2-(CH₂)₄-1,2-C₂B₁₁H₁₁ (**1a**). The results indicate that the carbon-chain linkage between the two cage carbon atoms does play an important role in the cage transformation reactions, which is detailed in this article.

RESULTS

Molecular Structures of 13-Vertex Carboranes **1a,b**.

Both **1a**⁴ and **1b**¹⁴ have been reported, yet their structures remain unknown. It is important to get structural parameters in order to compare the chemical properties between **1a** and **1b** and to study the role of carbon-chain length in reactivity. We then determined their single-crystal structures (Figure 1). Both adopt a heneicosahedral cage geometry, similar to those reported for 13-vertex carboranes.^{3,5,8} The cage C–C distance of 1.425(4) Å in **1a** is almost identical with that of 1.421(3) Å in **1b**. Other structural parameters are also very close to each other (see Table S1 in the Supporting Information).

Received: July 7, 2013

Published: August 26, 2013

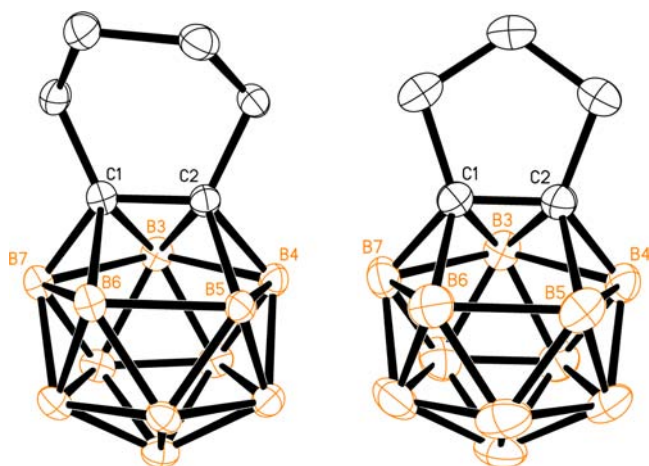
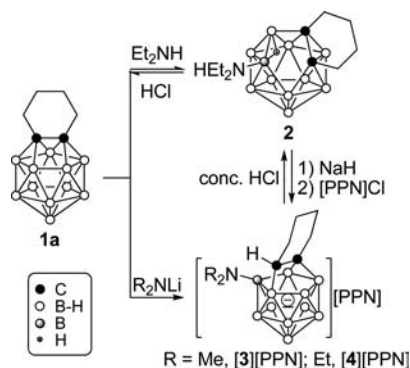


Figure 1. Molecular structures of **1a** (left) and **1b** (right).

Reaction of **1a** with Secondary Amine and Amide.

Though the cage geometries and structural parameters of **1a,b** are almost the same, they behave differently toward Et_2NH . Treatment of **1a** with excess Et_2NH in toluene at room temperature afforded, after recrystallization from CH_2Cl_2 , a 1:1 adduct *nido*-7- $\text{NEt}_2\text{H}-\mu-1,3-(\text{CH}_2)_4-1,3-\text{C}_2\text{B}_{11}\text{H}_{11}$ (**2**) in 88% isolated yield (Scheme 1), rather than the expected cage carbon extrusion products as observed in the reaction with **1b**.¹⁶

Scheme 1. Reactions of **1a** with Secondary Amine and Amide



The ^{11}B NMR spectrum of **2** exhibited a 2:2:4:2:1 pattern in the range 4.1 to -33 ppm. Its ^1H and ^{13}C NMR spectra exhibited relatively broad signals of the methylene groups attached to the N atom or the cage carbons. The solid-state structure of **2** was unambiguously confirmed by single-crystal X-ray analyses and is shown in Figure 2. The cage geometry can be viewed as a 13-vertex *nido*-cluster. Such a geometry is different from those of 13-vertex *nido*-carborane dianions formed by the reduction of a 13-vertex *closo*-carborane with group 1 metals.⁵ The NEt_2H group is bonded to the central boron atom of the C_2B_3 open face at a distance of 1.580(2) Å. This measured value is significantly longer than that of 1.414(11) Å in $[\mu-7,8,10-(\text{CH}_2)_3\text{CHB}(\text{NEt}_2)-7-\text{CB}_{10}\text{H}_{10}]^-$,¹⁶ and 1.398 Å in 6- R_2N -*nido*-5,7- $\text{C}_2\text{B}_8\text{H}_{11}$,¹⁸ but is very close to a normal B–N single bond.¹⁹ This conclusion is supported by the sum of angles around the N atom being 337.9°, indicative of a sp^3 -hybridized N atom. Thus, the hydrogen atom is still bonded to the N atom to form the zwitterionic salt of **2**.

Complex **2** might be the first intermediate in the cage carbon extrusion reaction of $\mu-1,2-(\text{CH}_2)_3-1,2-\text{C}_2\text{B}_{11}\text{H}_{11}$ (**1b**) as

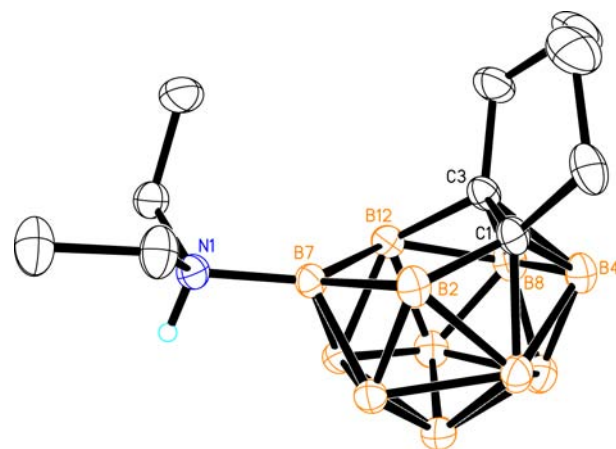


Figure 2. Molecular Structure of 7- $\text{NEt}_2\text{H}-\mu-1,3-(\text{CH}_2)_4-1,3-\text{C}_2\text{B}_{11}\text{H}_{11}$ (**2**).

proposed previously.¹⁶ Indeed, heating a C_6D_6 solution of **2** afforded a mixture of products from which the unique resonances of CB_{11}^- species could be identified. This result indicated that the 6- to 7-membered ring expansion was not as facile as that from a 5- to 6-membered one, as observed in the cage carbon extrusion reaction of **1b**.^{15,16}

Reactions of **1a** with secondary amides gave products with different cage geometry. Treatment of **1a** with 1 equiv of Me_2NLi in toluene followed by cation exchange with $[\text{PPN}]\text{Cl}$ ($\text{PPN} = \text{bis}(\text{triphenylphosphine})\text{iminium cation}$) afforded $[\text{9-NMe}_2-\mu-7,8,10-(\text{CH}_2)_4\text{CCH-B}_{11}\text{H}_{10}][\text{PPN}]$ (**[3][PPN]**) as pale yellow crystals in 91% isolated yield. On the other hand, when Et_2NLi was used as a nucleophile, a mixture of products containing about 60% of $[\text{9-NEt}_2-\mu-7,8,10-(\text{CH}_2)_4\text{CCH-B}_{11}\text{H}_{10}][\text{PPN}]$ (**[4][PPN]**) was obtained according to the ^{11}B NMR spectrum. Purification of **[4][PPN]** from the reaction mixture was not successful. However, when **2** was deprotonated by NaH in CH_2Cl_2 , **[4]⁻** was formed almost quantitatively as evidenced by ^{11}B NMR. Cation exchange with $[\text{PPN}]\text{Cl}$ followed by recrystallization from CH_2Cl_2 gave **[4][PPN]** as pale yellow crystals in 95% isolated yield. It was noteworthy that upon addition of an excess amount of conc. HCl , **[4]⁻** was quickly converted to **2** and finally to **1a** as evidenced by ^{11}B and ^1H NMR spectra (Scheme 1).

Complexes **[3][PPN]** and **[4][PPN]** were characterized by various spectroscopic data and elemental analyses. Their ^{11}B NMR spectra were almost identical, in which the downfield-shifted signal of the BNR_2 vertex was observed at about 50 ppm, comparing with that of 40 ppm in $[\mu-7,8,10-(\text{CH}_2)_3\text{CHB}(\text{NEt}_2)-7-\text{CB}_{10}\text{H}_{10}]^-$.¹⁶ The peaks of the $\alpha\text{-CH}$ were observed at 1.26 ppm for **[3]⁻** and 1.32 ppm for **[4]⁻** in the ^1H NMR spectra, and the corresponding ^{13}C signals were observed at 6.8 ppm and 8.5 ppm, respectively. These NMR data suggested the H-migration from the cage boron to the cage carbon.

Molecular structures of both **[3][PPN]** and **[4][PPN]** were confirmed by single-crystal X-ray analyses and the anions are shown in Figures 3 and 4, respectively. Their geometry can be viewed as an 11-vertex *nido*- B_{11} cluster capping with a bridging $(\text{CH}_2)_4\text{CCH}$ unit with the cage $\text{C}(1)-\text{C}(2)$ distance of 1.535(5) Å in **[3]⁻** and 1.542(6) Å in **[4]⁻** (Table 1). The $\text{N}(1)-\text{B}(9)$ distance of 1.405(5) Å in **[3]⁻** and $\text{N}(2)-\text{B}(9)$ distance of 1.411(6) Å in **[4]⁻** suggest a typical $\text{B}=\text{N}$ double bond.^{18,19} The sum of bond angles around the N atom of 359.7(4)° in **[3]⁻** and 360.0(4)° in **[4]⁻** confirms its sp^2

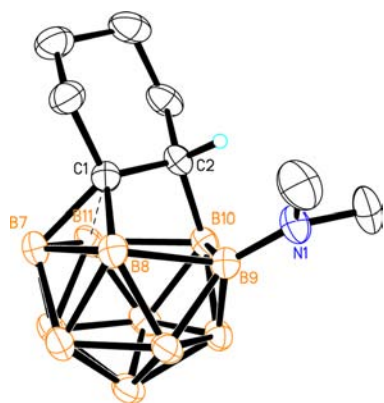


Figure 3. Molecular Structure of $[9\text{-NMe}_2\text{-}\mu\text{-}7,8,10\text{-(CH}_2)_4\text{CCH-B}_{11}\text{H}_{10}]^-$ ($[3]^-$) in $[3][\text{PPN}]$.

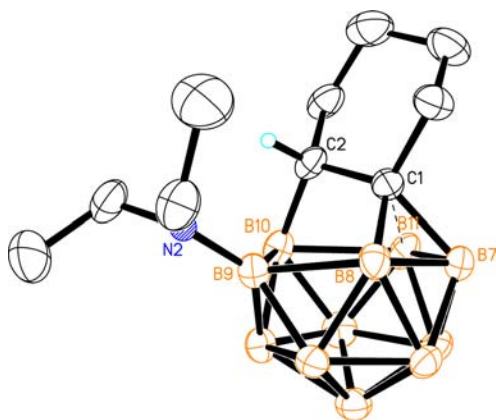


Figure 4. Molecular Structure of $[9\text{-NEt}_2\text{-}\mu\text{-}7,8,10\text{-(CH}_2)_4\text{CCH-B}_{11}\text{H}_{10}]^-$ ($[4]^-$) in $[4][\text{PPN}]$.

hybridization. These results are in very good agreement with the NMR data. Such a $\text{B}=\text{N}$ double bond formation promotes the H-migration from the cage boron to the carbon, resulting in the formation of $sp^3\text{-CH}$.

Reaction with MeOH. Reaction of **1a** with pure MeOH was not as facile as that of **1b**, and the reaction proceeded very slowly at room temperature. This reaction was closely monitored by ^1H and ^{11}B NMR spectra in CD_3OD . The formation of $[3\text{-OMe-}\mu\text{-}1,2\text{-(CH}_2)_4\text{-}1,2\text{-C}_2\text{B}_{11}\text{H}_{11}]^-$ ($[5]^-$) was observed, and resonances attributable to B(OMe)_3 and *closo*- CB_{11}^- anions appeared with the fade of **1a** and $[5]^-$ after four weeks. It was later found that the intermediate $[5]^-$ was almost immediately and quantitatively formed by adding weak base to the MeOH solution of **1a**. Treatment of **1a** with excess Et_3N or PS (Proton Sponge) in MeOH at room temperature gave a 13-vertex *nido*-carborane salt $[3\text{-OMe-}\mu\text{-}1,2\text{-(CH}_2)_4\text{-}1,2\text{-C}_2\text{B}_{11}\text{H}_{11}][\text{Et}_3\text{NH}]$ ($[5][\text{Et}_3\text{NH}]$) or $[5][\text{PSH}]$, respectively, in 90% yield (Scheme 2).

Both $[5][\text{Et}_3\text{NH}]$ and $[5][\text{PSH}]$ were characterized by various spectroscopic data and elemental analyses. Their ^{11}B NMR spectra exhibited a 1:2:1:4:2:1 pattern in the range 1.7 to -26.0 ppm with the chemical shift of BOMe vertex at 1.7 ppm. The cage carbons were found at about 141 ppm in the ^{13}C NMR spectra, which was close to that of 142.5 ppm observed in their parent complex **1a**.

The molecular structure of $[5][\text{Et}_3\text{NH}]$ was subject to X-ray analyses, but the resolution was low due to poor quality of single crystals (Figure S1 in the Supporting Information). High

quality single crystals of $[5][\text{PSH}]$ were grown from a THF solution, and the structure of the anion $[5]^-$ is shown in Figure 5. Its cage geometry does not represent any of the known 13-vertex *nido*-carborane dianions.^{1,5} It is produced by formally breaking two C–B bonds of the trapezoidal face of 13-vertex carborane **1a**. The resultant C_2B_4 face is bent with a dihedral angle of $119.4(3)^\circ$. The MeO group is attached to the 7-coordinate B(3) atom, which is not on the open face. The B–O distance of $1.437(5)$ Å is significantly longer than that of $1.377(5)$ Å observed in $[\mu\text{-}7,8,10\text{-(CH}_2)_3\text{CHB(OMe)-}7\text{-CB}_{10}\text{H}_{10}]^-$ formed from reaction of $\mu\text{-}1,2\text{-(CH}_2)_3\text{-}1,2\text{-C}_2\text{B}_{11}\text{H}_{11}$ (**1b**) with MeOH in the presence of PS.¹⁷ Such a long B–O distance suggests that the cage B(3) may not accept an electron pair from the O atom, so as to remain at seven degree vertex, which is greatly different from the known 13-vertex *nido*-carborane anions.⁵

Complex $[5][\text{Et}_3\text{NH}]$ is very stable at room temperature. However, upon heating in a MeOH solution in the presence of excess Et_3N at 70°C for 24 h in a sealed tube, a *nido*- CB_{10}^- salt, $[\mu\text{-}7,8\text{-(CH}_2)_4\text{CHB(OMe)}_2\text{-}7\text{-CB}_{10}\text{H}_{11}][\text{Et}_3\text{NH}]$ ($[6][\text{Et}_3\text{NH}]$), was formed. Cation exchange with PS gave $[\mu\text{-}7,8\text{-(CH}_2)_4\text{CHB(OMe)}_2\text{-}7\text{-CB}_{10}\text{H}_{11}][\text{PSH}]$ ($[6][\text{PSH}]$) as a white solid in 90% isolated yield (Scheme 2).

Complex $[6][\text{PSH}]$ was characterized by various NMR data and elemental analyses. Its spectroscopic properties were very similar to those of $[\mu\text{-}7,8\text{-(CH}_2)_3\text{CHB(OMe)}_2\text{-}7\text{-CB}_{10}\text{H}_{11}][\text{PSH}]$.¹⁷ The $^{11}\text{B}\{^1\text{H}\}$ NMR spectrum clearly exhibited a broad signal at 32.2 ppm attributable to the RB(OMe)_2 unit, a singlet at 0.6 ppm assignable to the RB vertex and other 9 doublets. The broad signal of $\alpha\text{-CH}$ was observed at 15.1 ppm in the ^{13}C NMR spectrum. A broad signal at -3.3 ppm with relative intensity of 2 was detected in the ^1H NMR spectrum, indicating two bridging H atoms on the 5-membered open face of the *nido*- CB_{10}^- anion.

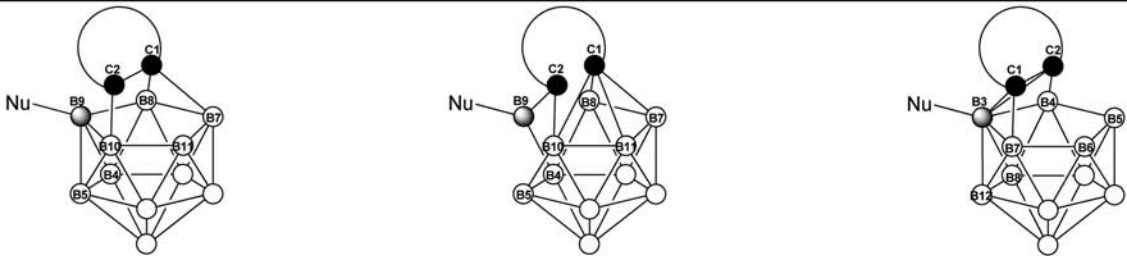
Single crystals of $[6][\text{PSH}]$ were grown from a THF solution. X-ray diffraction studies indicate that the anion adopts a similar structure to that of $[\mu\text{-}7,8\text{-(CH}_2)_3\text{CHB(OMe)}_2\text{-}7\text{-CB}_{10}\text{H}_{11}]^-$ (Figure 6).¹⁷ The *exo* boryl group takes up the *a*-position rather than the *e*-position in the twist-chair conformation of the 7-membered ring.

The B(OMe)_2 group in $[6]^-$ could be converted to other functional units. Treatment of $[6][\text{Et}_3\text{NH}]$, which was prepared in situ without further purification, with an excess amount of H_2O_2 , followed by cation exchange with PS, gave $[\mu\text{-}7,8\text{-(CH}_2)_4\text{CHOH-}7\text{-CB}_{10}\text{H}_{11}][\text{PSH}]$ ($[7][\text{PSH}]$) as a white powder in 90% isolated yield. On the other hand, reaction of $[6][\text{Et}_3\text{NH}]$ with an aqueous solution of Et_3N at 105°C for 24 h in a sealed tube, followed by cation exchange with PS, afforded the hydrolysis product $[\mu\text{-}7,8\text{-(CH}_2)_4\text{CHB(OH)}_2\text{-}7\text{-CB}_{10}\text{H}_{11}][\text{PSH}]$ ($[8][\text{PSH}]$) as a white solid in 50% isolated yield (Scheme 3).

The ^{11}B NMR spectrum of $[8][\text{PSH}]$ was almost the same as that of its parent boronic ester $[6][\text{PSH}]$. The ^1H and ^{13}C NMR spectra of $[6]^-$ and $[8]^-$ were also very similar, except for the peaks of MeO groups. On the other hand, a characteristic singlet of the RB vertex was detected at 0.3 ppm in the ^{11}B NMR spectrum of $[7][\text{PSH}]$, and no $(\text{MeO})_2\text{B}$ signal was observed. The $\alpha\text{-CH}$ proton was found at 3.41 ppm in the ^1H NMR spectrum of $[7]^-$, and the corresponding carbon was observed at 65.8 ppm.

Single-crystal X-ray analyses confirmed the molecular structure of $[7]^-$ (Figure 7). It has a very similar cage geometry to that of its parent complex $[6]^-$. The hydroxyl group takes up

Table 1. Selected Bond Lengths (Å) in $[9\text{-Nu-}\mu\text{-7,8,10-(CH}_2)_4\text{CCH-B}_{11}\text{H}_{10}]^-$, $[\mu\text{-7,8,10-(CH}_2)_3\text{CHB(Nu)-7-CB}_{10}\text{H}_{10}]^-$, and $[3\text{-OMe-}\mu\text{-1,2-(CH}_2)_4\text{-1,2-C}_2\text{B}_{11}\text{H}_{11}]^-$



	$[9\text{-NMe}_2\text{-}\mu\text{-7,8,10-(CH}_2)_4\text{CCH-B}_{11}\text{H}_{10}]^-$ ([3] ⁻)	$[9\text{-NEt}_2\text{-}\mu\text{-7,8,10-(CH}_2)_4\text{CCH-B}_{11}\text{H}_{10}]^-$ ([4] ⁻)	$[\mu\text{-7,8,10-(CH}_2)_3\text{CH-B(NEt}_2\text{)-7-CB}_{10}\text{H}_{10}]^-$ ^{a,b}	$[\mu\text{-7,8,10-(CH}_2)_3\text{CH-B(OMe)-7-CB}_{10}\text{H}_{10}]^-$ ^c	$[3\text{-OMe-}\mu\text{-1,2-(CH}_2)_4\text{-1,2-C}_2\text{B}_{11}\text{H}_{11}]^-$ ([5] ⁻)
C1-C2	1.535(5)	1.542(6)	2.660(13)	2.464(8)	C1-C2 1.390(5)
C1-B9	2.490(6)	2.544(7)	2.881(13)	2.594(8)	C2-B3 1.752(5)
C1-B8	1.683(6)	1.674(7)	1.750(10)	1.632(6)	C2-B4 1.564(6)
C1-B7	1.682(6)	1.683(7)	1.749(8)	1.654(8)	C2-B5 2.799(6)
C1-B11	2.059(6)	1.993(7)	1.731(9)	1.613(5)	C2-B6 3.216(6)
C1-B10	2.516(6)	2.517(7)	1.748(15)	1.843(8)	C2-B7 2.594(6)
C2-B9	2.366(6)	2.376(7)	1.568(13)	1.556(6)	C1-B3 1.755(6)
C2-B8	2.759(6)	2.737(7)	3.278(13)	2.894(8)	C1-B4 2.592(6)
C2-B7	2.929(6)	2.959(7)	4.061(13)	3.887(8)	C1-B5 3.214(6)
C2-B11	2.275(6)	2.274(7)	3.383(13)	3.287(8)	C1-B6 2.795(6)
C2-B10	1.631(6)	1.625(7)	1.704(11)	1.678(6)	C1-B7 1.560(5)
C2-B4	3.601(6)	3.579(7)	3.011(13)	2.914(8)	C1-B8 3.181(6)
C2-B5	3.103(6)	3.091(7)	2.002(13)	2.282(8)	C1-B12 2.765(6)
B9-B8	1.932(6)	1.966(8)	2.552(13)	2.036(7)	B3-B4 2.098(6)
B9-B10	2.063(6)	2.024(8)	2.498(13)	2.546(8)	B3-B7 2.124(6)
B9-B4	1.708(6)	1.693(8)	1.862(12)	1.778(6)	B3-B8 1.795(7)
B9-B5	1.721(6)	1.703(8)	1.787(15)	2.185(8)	B3-B12 1.805(6)
B9-Nu	1.405(5)	1.411(6)	1.414(11)	1.377(5)	B3-Nu 1.437(5)

^aSee ref 16. ^bAverage values of two crystallographic independent molecules in the unit cell. ^cSee ref 17.

the a-position in [7]⁻ in a chair conformation, which is the same as that observed in [6]⁻.

Reaction with (4-MeC₆H₄)SNa. Treatment of **1a** with 1 equiv of (4-MeC₆H₄)SNa in THF, followed by salt metathesis with [PPN]Cl, gave $[\mu\text{-1,2-(CH}_2)_4\text{CHS(4-MeC}_6\text{H}_4\text{)-1-CB}_{11}\text{H}_{10}][\text{PPN}]$ ([9][PPN]) in 80% isolated yield (Scheme 4). The ¹¹B NMR spectrum of the reaction mixture showed the formation of an intermediate that was very slowly converted to [9]⁻. Such a transformation was not completed even within a month. This process was, however, largely accelerated by heating the solution at 70 °C and completed in one day.

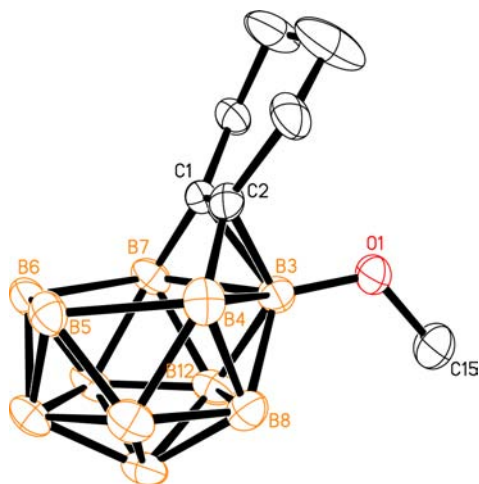
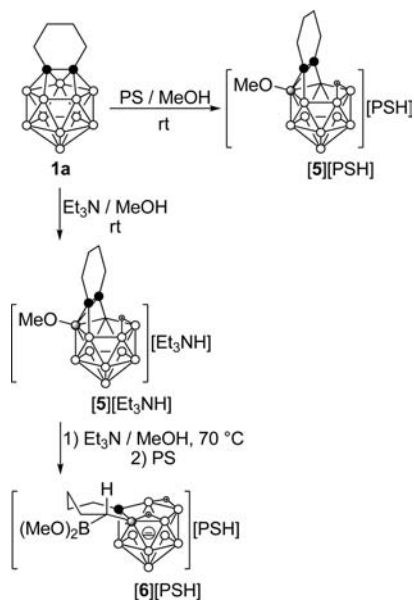
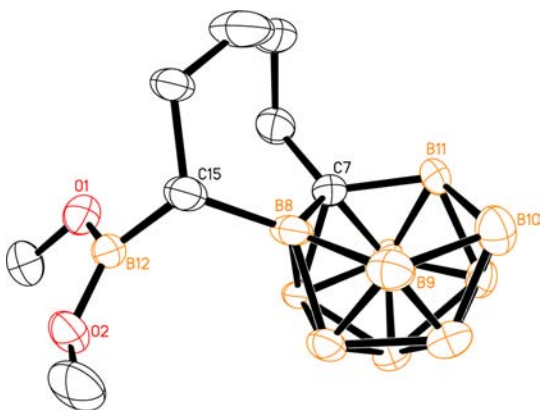
Complex [9][PPN] was fully characterized by various spectroscopic data and elemental analyses. Its spectroscopic features are very similar to those observed in $[\mu\text{-1,2-(CH}_2)_3\text{CHS(4-MeC}_6\text{H}_4\text{)-1-CB}_{11}\text{H}_{10}]^-$.¹⁶ The BR vertex was unambiguously assigned at -6.6 ppm as a singlet in the ¹¹B

NMR spectrum. The *exo* C atom bonded to the cage B was observed as a broad signal at 35.9 ppm in the ¹³C NMR spectrum. Single-crystal X-ray diffraction studies reveal that [9]⁻ shares common structural features with those of $[\mu\text{-1,2-(CH}_2)_3\text{CHNu-1-CB}_{11}\text{H}_{10}]^-$,^{15,16} as shown in Figure 8.

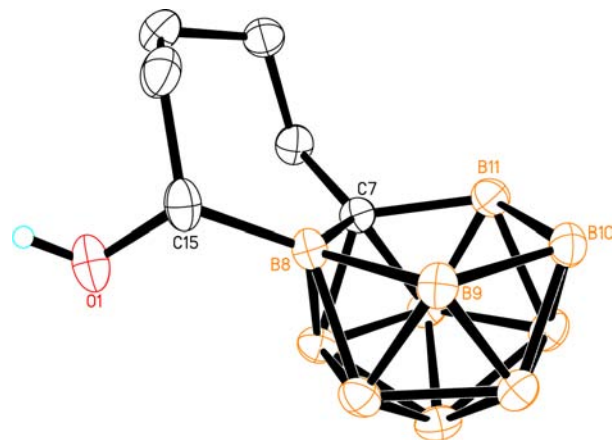
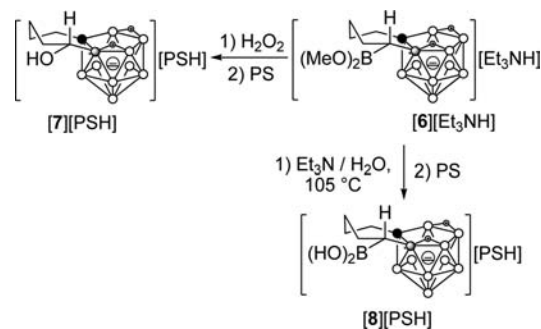
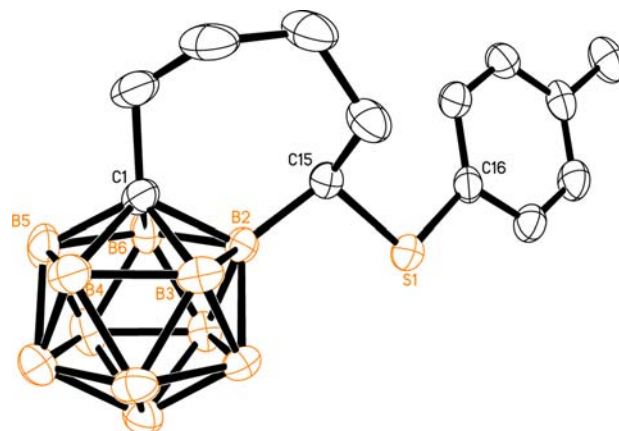
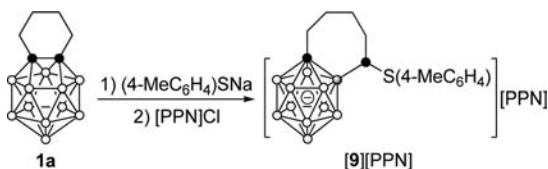
DISCUSSION

The above results showed that reaction of **1a** with hard nucleophiles such as Et₂NH, R₂NLi (R = Me, Et), and MeOH/base gave *nido*-carboranes [2]⁻-[5]⁻ with different cage structures from that of **1b**, $[\mu\text{-7,8,10-(CH}_2)_3\text{CHB(Nu)-7-CB}_{10}\text{H}_{10}]^-$ ([10]⁻) (Scheme 5). On the other hand, both **1a** and **1b** reacted with soft nucleophile (4-MeC₆H₄)SNa to afford the CB₁₁⁻ anions, $[\mu\text{-1,2-(CH}_2)_n\text{CHS(4-MeC}_6\text{H}_4\text{)-1-CB}_{11}\text{H}_{10}]^-$ (*n* = 4, [9]⁻; *n* = 3, [11]⁻), though they showed different reaction rates. It was noted that treatment of [2]⁻-

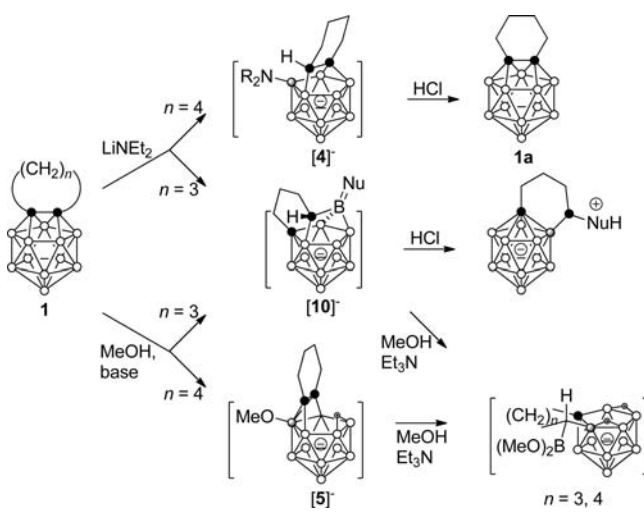
Scheme 2. Reactions of 1a with Basic MeOH

Figure 5. Molecular structure of [3-OMe- μ -1,2-(CH₂)₄-1,2-C₂B₁₀H₁₁][−] ([5][−]) in [5][PSH].Figure 6. Molecular structure of [μ -7,8-(CH₂)₄CHB(OMe)₂-7-CB₁₀H₁₁][−] ([6][−]) in [6][PSH].

[4][−] with concentrated HCl led to the recovery of 1a, whereas reaction of [10][−] with concentrated HCl resulted in the formation of the cage carbon extrusion product *closo*-CB₁₁[−]

Scheme 3. Oxidation and Hydrolysis of Boronic Ester [6][−]Figure 7. Molecular structure of [μ -7,8-(CH₂)₄CHOH-7-CB₁₀H₁₁][−] ([7][−]) in [7][PSH].Scheme 4. Reaction of 1a with (4-MeC₆H₄)SNaFigure 8. Molecular structure of [μ -1,2-(CH₂)₄CHS(4-MeC₆H₄)-1-CB₁₁H₁₀][−] ([9][−]) in [9][PPN].

monoanions.¹⁶ However, in the presence of base, [5][−] and [10][−] were all converted to the cage carbon/boron extrusion species *nido*-CB₁₀[−] monoanions. It is very obvious that carbon-chain length (CH₂)_{*n*} between two cage carbon atoms plays a

Scheme 5. Reactivity of 13-Vertex Carboranes **1a** and **1b** toward Nucleophiles

crucial role in the reactivity of 13-vertex carboranes and the product formation. These differences may be associated with the cage rearrangement that is restricted by the carbon-chain length (C,C'-linkage). For example, the ring expansion process from 5- to 6-membered ring is expected to be easier than that from 6- to 7-membered one. Thus, **1b** is more reactive than **1a** in the reaction with nucleophiles, leading to the formation of cage atom extrusion products. This can also explain the facile protonation of [2]⁻–[4]⁻ to form **1a**, rather than to the cage carbon extrusion products, thermodynamically more stable species *closo*-CB₁₁⁻ anions. It is anticipated that the rigidity of C,C'-linkages may have an impact on the reactivity of 13-vertex carboranes.

CONCLUSION

The experimental results clearly show that carbon-chain length between two cage carbon atoms has a great influence on the reactivity of 13-vertex carboranes toward nucleophiles, as well as the cage structures of the resultant compounds. Products with various cage geometries were obtained in the reaction of **1a** with hard nucleophiles such as Et₂NH, R₂NLi (R = Me, Et), and MeOH/base (base = Et₃N, PS), which is different from those of **1b**. Reaction of **1a** with a soft nucleophile like (4-MeC₆H₄)₂SNa gives cage carbon extrusion species CB₁₁⁻ anion, similar to that of **1b**, although the reaction rate is much slower. These observations may be ascribed to the restrictions imposed by the carbon-chain length, which limits the cage transformation, resulting in the formation of various cage geometries.

EXPERIMENTAL SECTION

General Procedures. Unless otherwise noted, all experiments were performed under an atmosphere of dry dinitrogen or argon with the rigid exclusion of air and moisture using standard Schlenk techniques or in a glovebox. CH₂Cl₂ was refluxed over CaH₂ for several days and distilled immediately prior to use. Other organic solvents were refluxed over sodium benzophenone ketyl for several days and freshly distilled prior to use. 13-Vertex carboranes μ-1,2-(CH₂)_n-1,2-C₂B₁₀H₁₀ (*n* = 4, **1a**; *n* = 3, **1b**) were prepared according to literature methods.^{4,14} X-ray-quality crystals of both **1a** and **1b** were obtained by slow evaporation of a saturated *n*-hexane solution. All other chemicals were purchased from either Aldrich or Acros Chemical Company and used as received unless otherwise noted. Infrared

spectra were obtained from KBr pellets on a Perkin-Elmer 1600 Fourier transform spectrometer. The ¹H and ¹³C NMR spectra were recorded on a Bruker DPX 400 spectrometer at 400 and 100 MHz, respectively. The ¹¹B NMR spectra were recorded on a Bruker DPX 300 spectrometer at 96 MHz, or a Bruker DPX 400 spectrometer at 128 MHz, respectively. All chemical shifts were reported in δ units with references to the residual protons or carbons of the deuterated solvents for proton or carbon chemical shifts, and to external BF₃·OEt₂ (0.0 ppm) for boron chemical shifts. Mass spectra were recorded on a Thermo Finnigan MAT 95 XL spectrometer. Elemental analyses were performed by MEDAC Ltd., Brunel University, Middlesex, U.K., or the Shanghai Institute of Organic Chemistry, the Chinese Academy of Sciences, Shanghai, China.

Preparation of 7-NEt₂H-μ-1,3-(CH₂)₄-1,3-C₂B₁₁H₁₁ (2**).** To a toluene (10 mL) solution of **1a** (420 mg, 2.00 mmol) was added Et₂NH (2.0 mL, 1.41 g, 19.4 mmol), and the solution was stirred at room temperature overnight. After removal of the volatile materials, the pale yellow residue was recrystallized from CH₂Cl₂/*n*-hexane to afford **2** as colorless crystals (500 mg, 88%). ¹H NMR (400 MHz, CD₂Cl₂): δ 3.24 (br, 4H, NCH₂), 2.24 (br, 2H, CCH₂), 2.11 (m, 2H, CCH₂), 1.63 (br, 4H, CCH₂CH₂), 1.38 (t, *J* = 7.3 Hz, 6H, CH₃), -0.21 (br, 1H, μ-H). ¹³C{¹H} NMR (100 MHz, CD₂Cl₂): δ 45.9 (NCH₂), 38.1 (br, CCH₂), 21.9 (CCH₂CH₂), 10.4 (CH₃), the cage carbons were not observed. ¹¹B NMR (96 MHz, CD₂Cl₂): δ 4.1 (d+d, *J*_{BH(1)} = 73 Hz, *J*_{BH(2)} ≈ 120 Hz, 2B), -5.7 (d, *J*_{BH} = 140 Hz, 2B), -16.9 (d, *J*_{BH} = 142 Hz, 4B), -24.8 (d, *J*_{BH} = 142 Hz, 2B), -33.0 (br, unresolved, 1B). IR (KBr, cm⁻¹): ν_{max} 2580 (B–H). Anal. Calcd for C₁₀H₃₀B₁₁N (2): C, 42.40; H, 10.67; N, 4.94. Found: C, 42.70; H, 10.42; N, 5.01.

Preparation of [9-NMe₂-μ-7,8,10-(CH₂)₄CCH-B₁₁H₁₀][PPN] ([3**]-[PPN]).** To a toluene (10 mL) solution of **1a** (105 mg, 0.50 mmol) was added LiNMe₂ (26 mg, 0.50 mmol) at -30 °C, and the solution was stirred at room temperature overnight. After addition of [PPN]Cl (287 mg, 0.50 mmol), the suspension was further stirred at room temperature for 6 h. After removal of the solvent, the residue was extracted with CH₂Cl₂ (2 × 5 mL). Recrystallization from CH₂Cl₂/*n*-hexane gave [**3**][PPN] as pale yellow crystals (360 mg, 91%). ¹H NMR (400 MHz, CD₂Cl₂): δ 7.69 (m, 6H, PPN), 7.51 (m, 24H, PPN), 3.00 (s, 6H, NCH₃), 1.88 (m, 1H, CH₂), 1.81 (m, 3H, CH₂), 1.67 (m, 1H, CH₂), 1.54 (m, 2H, CH₂), 1.45 (m, 1H, CH₂), 1.26 (m, 1H, α-CH). ¹³C{¹H} NMR (100 MHz, CD₂Cl₂): δ 134.1, 132.4, 129.8, 127.3 (PPN), 63.5 (cage C), 51.8 (CH₂), 43.5 (NCH₃), 40.5 (CH₂), 28.8 (CH₂), 25.2 (CH₂), 6.8 (α-CH). ¹¹B NMR (96 MHz, CD₂Cl₂): δ 48.8 (s, 1B), 25.5 (d, *J*_{BH} = 103 Hz, 1B), 9.6 (d, *J*_{BH} = 131 Hz, 1B), -6.8 (d, *J*_{BH} = 117 Hz, 1B), -8.6 (d, *J*_{BH} = 146 Hz, 1B), -11.1 (d, *J*_{BH} = 137 Hz, 1B), -18.5 (d, *J*_{BH} = 131 Hz, 1B), -20.3 (d, *J*_{BH} = 136 Hz, 1B), -23.0 (d, *J*_{BH} = 134 Hz, 2B), -32.6 (d, *J*_{BH} = 138 Hz, 1B). IR (KBr, cm⁻¹): ν_{max} 2502 (B–H), 2406 (B=N). Anal. Calcd for C₄₄H₅₅B₁₁N₂P₂ ([**3**][PPN]): C, 66.66; H, 6.99; N, 3.53. Found: C, 66.69; H, 7.26; N, 3.15.

Preparation of [9-NEt₂-μ-7,8,10-(CH₂)₄CCH-B₁₁H₁₀][PPN] ([4**]-[PPN]).** To a CH₂Cl₂ (10 mL) solution of **2** (283 mg, 1.00 mmol) was added excess NaH (80 mg, 3.30 mmol) at room temperature, and the suspension was stirred for 2 h until no gas was evolved. After addition of [PPN]Cl (287 mg, 0.50 mmol), the suspension was further stirred for 6 h. The clear solution was concentrated to about 10 mL, and *n*-hexane layering gave [**4**][PPN] as pale yellow crystals (390 mg, 95%). ¹H NMR (400 MHz, CD₂Cl₂): δ 7.69 (m, 6H, PPN), 7.52 (m, 24H, PPN), 3.47 (br, 1H, NCH₂), 3.28 (m, 3H, NCH₂), 1.81 (m, 4H, CH₂), 1.61 (m, 2H, CH₂), 1.50 (m, 1H, CH₂), 1.47 (m, 1H, CH₂), 1.32 (m, 1H, α-CH), 1.13 (br, 6H, CH₃). ¹³C{¹H} NMR (100 MHz, CD₂Cl₂): δ 134.1, 132.4, 129.8, 127.3 (PPN), 60.7 (cage C), 51.2 (CH₂), 46.2, 46.1 (NCH₂), 40.1 (CH₂), 29.0 (CH₂), 25.1 (CH₂), 15.6, 15.3 (CH₃), 8.5 (α-CH). ¹¹B NMR (96 MHz, CD₂Cl₂): δ 49.4 (s, 1B), 24.6 (d, *J*_{BH} = 103 Hz, 1B), 9.8 (d, *J*_{BH} = 126 Hz, 1B), -7.2 (d, *J*_{BH} = 125 Hz, 1B), -8.8 (d, *J*_{BH} = 146 Hz, 1B), -11.6 (d, *J*_{BH} = 136 Hz, 1B), -18.2 (d, *J*_{BH} = 134 Hz, 1B), -20.7 (d, *J*_{BH} = 130 Hz, 1B), -22.9 (d, *J*_{BH} = 130 Hz, 2B), -32.7 (d, *J*_{BH} = 136 Hz, 1B). IR (KBr, cm⁻¹): ν_{max} 2494 (B–H), 2417 (B=N). Anal. Calcd for C₄₆H₅₉B₁₁N₂P₂

([4][PPN]): C, 67.31; H, 7.24; N, 3.41. Found: C, 67.47; H, 7.31; N, 3.30.

Preparation of [3-Ome- μ -1,2-(CH₂)₄-1,2-C₂B₁₁H₁₁][Et₃NH] ([5]-[Et₃NH]). A mixture of Et₃N (726 mg, 7.20 mmol) and MeOH (10 mL) was added to **1a** (105 mg, 0.50 mmol) at 0 °C. The solution was stirred at room temperature for 5 min to give a MeOH solution of [5][Et₃NH]. After removal of the volatile materials, the residue was thoroughly washed with Et₂O to afford [5][Et₃NH] as a white solid (191 mg, 90%). X-ray-quality crystals were obtained by recrystallization from CH₂Cl₂. ¹H NMR (400 MHz, CD₂Cl₂): δ 6.17 (s, 1H, NH), 3.29 (t, *J* = 7.3 Hz, 6H, NCH₃), 3.21 (s, 3H, OCH₃), 2.79 (m, 2H, CCH₂), 2.59 (m, 2H, CCH₂), 1.58 (m, 4H, CCH₂CH₂), 1.42 (d, *J* = 7.3 Hz, 9H, CH₃). ¹³C{¹H} NMR (100 MHz, CD₂Cl₂): δ 141.1 (cage C), 52.4 (OCH₃), 48.6 (NCH₂), 36.3 (CCH₂), 23.3 (CCH₂CH₂), 9.3 (CH₃). ¹¹B NMR (128 MHz, CD₂Cl₂): δ 1.7 (s, 1B), -3.4 (d, *J*_{BH} = 112 Hz, 2B), -6.2 (d, *J*_{BH} = 142 Hz, 1B), -8.6 (d, *J*_{BH} = 116 Hz, 4B), -19.0 (d, *J*_{BH} = 130 Hz, 2B), -26.0 (d, *J*_{BH} = 139 Hz, 1B). IR (KBr, cm⁻¹): ν_{\max} 2511 (B-H). Anal. Calcd for C₁₃H₃₈B₁₁NO ([5]-[Et₃NH]): C, 45.47; H, 11.15; N, 4.08. Found: C, 45.28; H, 11.26; N, 4.24.

Preparation of [3-Ome- μ -1,2-(CH₂)₄-1,2-C₂B₁₁H₁₁][PSH] ([5]-[PSH]). Compound **1a** (105 mg, 0.50 mmol) was added to a 0.25 M PS solution in MeOH (10.0 mL, 2.5 mmol) at room temperature, giving a white suspension in 5 min. After removal of the volatile materials, the residue was thoroughly washed with Et₂O to afford [5][PSH] as a white solid (206 mg, 90%). X-ray-quality crystals were obtained by recrystallization from CH₂Cl₂. ¹H NMR (400 MHz, CD₂Cl₂): δ 8.04 (d, *J* = 8.2 Hz, 2H, C₁₀H₆), 7.86 (d, *J* = 7.5 Hz, 2H, C₁₀H₆), 7.74 (d, *J* = 7.9 Hz, 2H, C₁₀H₆), 3.23 (d, *J* = 1.6 Hz, 12H, NCH₃), 3.21 (s, 3H, OCH₃), 2.79 (m, 2H, CCH₂), 2.60 (m, 2H, CCH₂), 1.57 (m, 4H, CCH₂CH₂). ¹³C{¹H} NMR (100 MHz, CD₂Cl₂): δ 143.9 (C₁₀H₆), 140.5 (cage C), 135.8, 130.1, 127.6, 121.7, 118.9 (C₁₀H₆), 52.3 (OCH₃), 46.9 (NCH₃), 36.2 (CCH₂), 23.4 (CCH₂CH₂). ¹¹B NMR (128 MHz, CD₂Cl₂): δ 1.7 (s, 1B), -3.4 (d, *J*_{BH} = 109 Hz, 2B), -6.1 (d, *J*_{BH} = 136 Hz, 1B), -8.6 (d, *J*_{BH} = 123 Hz, 4B), -19.0 (d, *J*_{BH} = 132 Hz, 2B), -26.0 (d, *J*_{BH} = 139 Hz, 1B). IR (KBr, cm⁻¹): ν_{\max} 2508 (B-H). Anal. Calcd for C₂₂H₄₁B₁₁N₂O ([5][PSH]): C, 55.25; H, 9.05; N, 6.14. Found: C, 54.98; H, 8.84; N, 6.10.

Preparation of [μ -7,8-(CH₂)₄CHB(OMe)₂-7-CB₁₀H₁₁][PSH] ([6]-[PSH]). A MeOH (10 mL) solution of [5][Et₃NH], which was prepared in situ from Et₃N (726 mg, 7.2 mmol) and **1a** (105 mg, 0.50 mmol), was heated at 70 °C for 24 h to give a solution of [6][Et₃NH]. A 0.25 M PS solution in MeOH (10.0 mL, 2.5 mmol) was added. After removal of the volatile materials, the residue was thoroughly washed with Et₂O to afford [6][PSH] as a white solid (220 mg, 90%). X-ray-quality crystals were obtained by recrystallization from THF. ¹H NMR (400 MHz, CD₂Cl₂): δ 8.05 (d, *J* = 8.3 Hz, 2H, C₁₀H₆), 7.84 (d, *J* = 7.6 Hz, 2H, C₁₀H₆), 7.74 (d, *J* = 7.9 Hz, 2H, C₁₀H₆), 3.49 (s, 6H, OCH₃), 3.21 (d, *J* = 2.7 Hz, 12H, NCH₃), 2.07 (m, 1H, ϵ -CH₂), 1.90 (m, 1H, ϵ -CH₂), 1.81 (m, 1H, γ -CH₂), 1.71 (m, 1H, β -CH₂), 1.56 (m, 2H, δ -CH₂), 1.49 (m, 1H, β -CH₂), 1.31 (m, 1H, γ -CH₂), 0.85 (m, 1H, α -CH), -3.29 (br, 2H, μ -H). ¹³C{¹H} NMR (100 MHz, CD₂Cl₂): δ 143.8, 135.8, 130.1, 127.6, 121.7, 118.9 (C₁₀H₆), 57.4 (cage C), 51.2 (OCH₃), 46.9 (NCH₃), 37.6 (ϵ -CH₂), 31.0 (γ -CH₂), 30.3 (δ -CH₂), 28.7 (β -CH₂), 14.9 (br, α -CH). ¹¹B NMR (128 MHz, CD₂Cl₂): δ 32.2 (s, 1B), 0.6 (s, 1B), -4.2 (d, *J*_{BH} = 120 Hz, 1B), -9.2 (d, *J*_{BH} = 140 Hz, 2B), -10.8 (d, *J*_{BH} = 189 Hz, 1B), -23.8 (d, *J*_{BH} = 92 Hz, 2B), -26.4 (d, *J*_{BH} = 131 Hz, 1B), -30.1 (d, *J*_{BH} = 136 Hz, 1B), -33.9 (d, *J*_{BH} = 134 Hz, 1B). IR (KBr, cm⁻¹): ν_{\max} 2519 (B-H). Anal. Calcd for C₂₂H₄₅B₁₁N₂O₂ ([6][PSH]): C, 54.09; H, 9.28; N, 5.73. Found: C, 53.92; H, 9.13; N, 6.23.

Preparation of [μ -7,8-(CH₂)₄CHOH-7-CB₁₀H₁₁][PSH] ([7][PSH]). To a MeOH (10 mL) solution of [6][Et₃NH], which was prepared in situ from Et₃N (726 mg, 7.2 mmol) and **1a** (105 mg, 0.50 mmol), was added H₂O₂ (1.0 mL, 30%, 8.8 mmol) at 0 °C. The mixture was stirred at room temperature for 1 h. A 0.25 M PS solution in MeOH (10.0 mL, 2.5 mmol) was added. After removal of the volatile materials, the residue was thoroughly washed with Et₂O to afford [7][PSH] as a white solid (195 mg, 90%). X-ray-quality crystals were obtained by

recrystallization from CH₂Cl₂. ¹H NMR (400 MHz, CD₂Cl₂): δ 8.04 (dd, *J*₁ = 8.3 Hz, *J*₂ = 0.8 Hz, 2H, C₁₀H₆), 7.81 (dd, *J*₁ = 7.6 Hz, *J*₂ = 0.9 Hz, 2H, C₁₀H₆), 7.73 (t, *J* = 7.9 Hz, 2H, C₁₀H₆), 3.41 (d, *J* = 8.4 Hz, 1H, α -CH), 3.19 (d, *J* = 2.7 Hz, 12H, NCH₃), 2.04 (m, 1H, ϵ -CH₂), 1.92 (m, 1H, β -CH₂), 1.77 (m, 1H, ϵ -CH₂), 1.68 (m, 1H, δ -CH₂), 1.66 (m, 1H, γ -CH₂), 1.53 (m, 1H, β -CH₂), 1.46 (m, 1H, γ -CH₂), 1.36 (m, 1H, δ -CH₂), -3.40 (br, 2H, μ -H). ¹³C{¹H} NMR (100 MHz, CD₂Cl₂): δ 143.8, 135.9, 130.2, 127.6, 121.6, 118.9 (C₁₀H₆), 65.7 (α -CH), 55.9 (cage C), 46.9 (NCH₃), 40.8 (ϵ -CH₂), 37.7 (β -CH₂), 30.9 (δ -CH₂), 26.8 (γ -CH₂). ¹¹B NMR (128 MHz, CD₂Cl₂): δ 0.3 (s, 1B), -3.5 (d, *J*_{BH} = 123 Hz, 1B), -9.3 (unresolved, 3B), -23.6 (unresolved, 1B), -24.3 (unresolved, 1B), -26.7 (d, *J*_{BH} = 139 Hz, 1B), -30.7 (d, *J*_{BH} = 143 Hz, 1B), -32.9 (d, *J*_{BH} = 132 Hz, 1B). IR (KBr, cm⁻¹): ν_{\max} 2518, 2495 (B-H). Anal. Calcd for C₂₀H₄₀B₁₀N₂O ([7][PSH]): C, 55.52; H, 9.32; N, 6.47. Found: C, 55.55; H, 9.57; N, 6.40.

Preparation of [μ -7,8-(CH₂)₄CHB(OH)₂-7-CB₁₀H₁₁][PSH] ([8][PSH]). A MeOH (10 mL) solution of [6][Et₃NH] was prepared in situ from Et₃N (726 mg, 7.2 mmol) and **1a** (105 mg, 0.50 mmol). After removal of the volatile materials, Et₃N (726 mg, 7.2 mmol) and H₂O (10 mL) were added. The mixture was heated at 105 °C in a sealed tube for 24 h. A 0.25 M PS solution in MeOH (10 mL, 2.5 mmol) was then added. After removal of the volatile materials, the residue was thoroughly washed with Et₂O to give [8][PSH] as a white solid (115 mg, 50%). ¹H NMR (400 MHz, CD₂Cl₂): δ 8.04 (d, *J* = 8.2 Hz, 2H, C₁₀H₆), 7.83 (d, *J* = 7.5 Hz, 2H, C₁₀H₆), 7.73 (t, *J* = 7.9 Hz, 2H, C₁₀H₆), 4.97 (brs, 2H, OH), 3.19 (d, *J* = 2.6 Hz, 2H, NCH₃), 1.99 (m, 1H, ϵ -CH₂), 1.89 (m, 1H, β -CH₂), 1.72 (m, 1H, ϵ -CH₂), 1.66 (m, 1H, δ -CH₂), 1.62 (m, 2H, γ -CH₂), 1.46 (m, 1H, β -CH₂), 1.41 (m, 1H, δ -CH₂), 0.70 (br, 1H, α -CH), -3.31 (br, 2H, μ -H). ¹³C{¹H} NMR (100 MHz, CD₂Cl₂): δ 143.7, 135.8, 130.1, 127.6, 121.6, 118.9 (C₁₀H₆), 57.6 (cage C), 46.9 (NCH₃), 40.9 (ϵ -CH₂), 31.7 (δ -CH₂), 31.4 (γ -CH₂), 31.0 (β -CH₂), 18.7 (α -CH). ¹¹B NMR (128 MHz, CD₂Cl₂): δ 33.6 (s, 1B), 1.5 (s, 1B), -4.3 (d, *J*_{BH} = 116 Hz, 1B), -8.0 (d, *J*_{BH} = 138 Hz, 1B), -8.8 (d, *J*_{BH} = 141 Hz, 1B), -10.6 (d, *J*_{BH} \approx 228 Hz, 1B), -23.5 (d, *J*_{BH} = 96 Hz, 2B), -26.3 (d, *J*_{BH} = 129 Hz, 1B), -30.2 (d, *J*_{BH} = 129 Hz, 1B), -33.8 (d, *J*_{BH} = 135 Hz, 1B). IR (KBr, cm⁻¹): ν_{\max} 2514 (B-H). Anal. Calcd for C₂₂H₄₁B₁₁N₂O₂ ([8][PSH]): C, 52.17; H, 8.97; N, 6.08. Found: C, 52.20; H, 8.60; N, 5.90.

Preparation of [μ -1,2-(CH₂)₄CHS(4-Me-C₆H₅)-1-CB₁₁H₁₀][PPN] ([9][PPN]). To a THF (10 mL) solution of **1a** (105 mg, 0.50 mmol) was added (4-Me-C₆H₅)SNa (73 mg, 0.50 mmol), and the mixture was heated at 70 °C overnight. [PPN]Cl (287 mg, 0.50 mmol) was then added, and the mixture was further stirred for 6 h. After filtration, the colorless solution was concentrated to about 3 mL, to which was added DME (5 mL). *n*-Hexane layering afforded [9][PPN] as colorless crystals (350 mg, 80%). ¹H NMR (400 MHz, CD₂Cl₂): δ 7.69 (m, 6H, PPN), 7.52 (m, 24H, PPN), 7.22 (d, *J* = 8.1 Hz, 2H, C₆H₄), 7.04 (d, *J* = 8.0 Hz, 2H, C₆H₄), 3.10 (d, *J* = 8.1 Hz, 1H, α -CH), 2.28 (s, 3H, CH₃), 2.15 (m, 1H, ϵ -CH₂), 2.04 (m, 1H, ϵ -CH₂), 1.90 (m, 1H, β -CH₂), 1.77 (m, 2H, β -CH₂ + γ -CH₂), 1.53 (m, 2H, δ -CH₂), 1.19 (m, 1H, γ -CH₂). ¹³C{¹H} NMR (100 MHz, CD₂Cl₂): δ 136.6, 134.6 (C₆H₄), 134.0, 132.4, 129.8 (PPN), 129.47, 129.44 (C₆H₄), 127.3 (PPN), 71.8 (cage C), 40.6 (ϵ -CH₂), 35.7 (br, α -CH), 32.8 (β -CH₂), 29.7 (γ -CH₂), 27.3 (δ -CH₂), 21.0 (CH₃). ¹¹B NMR (128 MHz, CD₂Cl₂): δ -6.6 (s, 1B), -9.9 (d, *J*_{BH} = 148 Hz, 1B), -11.8 (d, *J*_{BH} = 135 Hz, 5B), -15.2 (d, *J*_{BH} = 131 Hz, 4B). IR (KBr, cm⁻¹): ν_{\max} 2541, 2527 (B-H). Calcd for C₄₉H₅₆B₁₁N₂S ([9][PPN]): C, 67.50; H, 6.47; N, 1.61. Found: C, 67.23; H, 6.55; N, 1.38.

X-ray Structure Determination. All single crystals were immersed in Paratone-N oil and sealed under N₂ in thin-walled glass capillaries. Data were collected on a Bruker SMART 1000 CCD diffractometer or a Bruker AXS Kappa Apex II Duo diffractometer using Mo K α radiation. An empirical absorption correction was applied using the SADABS program.²⁰ All structures were solved by direct methods and subsequent Fourier difference techniques and refined anisotropically for all non-hydrogen atoms by full-matrix least-squares calculations on *F*² using SHELXTL.²¹ The hydrogen atoms were geometrically fixed using the riding model. [9][PPN] showed

one THF of solvation. Crystal data and details of data collection and structure refinements are included in the Supporting Information.

■ ASSOCIATED CONTENT

■ Supporting Information

Crystallographic data in CIF format for **1a**, **1b**, **2**, [3][PPN], [4][PPN], [5][PSH], [6][PSH], [7][PSH], and [9][PPN]·THF, selected bond lengths and angles in **1a** and **1b**, crystal data and summary of data collection and refinement for **1a**, **1b**, **2**, [3][PPN], [4][PPN], [5][Et₃NH], [5][PSH], [6][PSH], [7][PSH], and [9][PPN]·THF, and molecular structure of [5][Et₃NH]. This material is available free of charge via the Internet at <http://pubs.acs.org>.

■ AUTHOR INFORMATION

Corresponding Author

*Fax: (852)26035057. E-mail: zxie@cuhk.edu.hk

Notes

The authors declare no competing financial interest.

■ ACKNOWLEDGMENTS

The work described in this paper was supported by grants from the Research Grants Council of the Hong Kong Special Administration Region (Project Nos. CUHK7/CRF/12G and 403912) and the National Basic Research Program of China (973 Program, Grant No. 2012CB821600). We thank Hoi-Shan Chan for single-crystal X-ray analyses.

■ REFERENCES

- (1) (a) Deng, L.; Xie, Z. *Coord. Chem. Rev.* **2007**, *251*, 2452–2476. (b) Deng, L.; Xie, Z. *Organometallics* **2007**, *26*, 1832–1845. (c) Zhang, J.; Xie, Z. *Chem.—Asian J.* **2010**, *5*, 1742–1757. (d) Zhang, J.; Xie, Z. *Pure Appl. Chem.* **2013**, *85*, 661–670. (e) Roy, D. K.; Bose, S. K.; Anju, R. S.; Mondal, B.; Ramkumar, V.; Ghosh, S. *Angew. Chem., Int. Ed.* **2013**, *52*, 3222–3226. (f) Roy, D. K.; Mondal, B.; Shankhari, P.; Anju, R. S.; Geetharani, K.; Mobin, S. M.; Ghosh, S. *Inorg. Chem.* **2013**, *52*, 6705–6712.
- (2) (a) Bregadze, V. I. *Chem. Rev.* **1992**, *92*, 209–223. (b) Saxena, A. K.; Maguire, J. A.; Hosmane, N. S. *Chem. Rev.* **1997**, *97*, 2421–2461. (c) Davidson, M.; Hughes, A. K.; Marder, T. B.; Wade, K. *Contemporary Boron Chemistry*; RSC: Cambridge, U.K., 2000. (d) Xie, Z. *Acc. Chem. Res.* **2003**, *36*, 1–9. (e) Bubnov, Y. N. *Boron Chemistry at the Beginning of the 21st Century*; Russian Academy of Sciences: Moscow, Russia, 2003. (f) Xie, Z. *Coord. Chem. Rev.* **2006**, *250*, 259–272. (g) Fox, M. A. In *Comprehensive Organometallic Chemistry III*; Crabtree, R. H., Mingos, D. M. P., Eds.; Elsevier: Oxford, 2007; Vol. 3, pp 49–112. (h) Shen, H.; Xie, Z. *Chem. Commun.* **2009**, 2431–2445. (i) Grimes, R. N. *Carboranes*, 2nd ed.; Academic Press: New York, 2011. (j) Qiu, Z.; Ren, S.; Xie, Z. *Acc. Chem. Res.* **2011**, *44*, 299–309. (k) Hosmane, N. S. *Boron Science: New Technologies and Applications*; CRC Press: Boca Raton, FL, 2011.
- (3) Burke, A.; Ellis, D.; Giles, B. T.; Hodson, B. E.; Macgregor, S. A.; Rosair, G. M.; Welch, A. J. *Angew. Chem., Int. Ed.* **2003**, *42*, 225–228.
- (4) Deng, L.; Chan, H.-S.; Xie, Z. *Angew. Chem., Int. Ed.* **2005**, *44*, 2128–2131.
- (5) Deng, L.; Chan, H.-S.; Xie, Z. *J. Am. Chem. Soc.* **2006**, *128*, 5219–5230.
- (6) Deng, L.; Zhang, J.; Chan, H.-S.; Xie, Z. *Angew. Chem., Int. Ed.* **2006**, *45*, 4309–4313.
- (7) McIntosh, R. D.; Ellis, D.; Rosair, G. M.; Welch, A. J. *Angew. Chem., Int. Ed.* **2006**, *45*, 4313–4316.
- (8) Zhang, J.; Deng, L.; Chan, H.-S.; Xie, Z. *J. Am. Chem. Soc.* **2007**, *129*, 18–19.
- (9) (a) Zi, G.; Li, H.-W.; Xie, Z. *Organometallics* **2001**, *20*, 3836–3838. (b) Zi, G.; Li, H.-W.; Xie, Z. *Chem. Commun.* **2001**, 1110–1111. (c) Zi, G.; Li, H.-W.; Xie, Z. *Organometallics* **2002**, *21*, 5415–5427.

(d) Deng, L.; Cheung, M.-S.; Chan, H.-S.; Xie, Z. *Organometallics* **2005**, *24*, 6244–6249.

(10) (a) Zakharkin, L. I.; Kalinin, V. N. *Russ. Chem. Bull.* **1965**, 1311. (b) Potenza, J. A.; Lipscomb, W. N.; Vickers, G. D.; Schroeder, H. J. *Am. Chem. Soc.* **1966**, *88*, 628–629. (c) Stanko, V. I.; Struchkov, Yu. T.; Klimova, A. I.; Bryukhova, L. V.; Semin, G. K. *Russ. J. Gen. Chem.* **1966**, *36*, 1707. (d) Andrews, J. S.; Zayas, J.; Jones, M., Jr. *Inorg. Chem.* **1985**, *24*, 3715–3716. (e) Zheng, Z.; Jiang, W.; Zinn, A. A.; Knobler, C. B.; Hawthorne, M. F. *Inorg. Chem.* **1995**, *34*, 2095–2100. (f) Reed, C. A. *Acc. Chem. Res.* **1998**, *32*, 133–139. (g) Körbe, S.; Schreiber, P. J.; Michl, J. *Chem. Rev.* **2006**, *106*, 5208–5249. (h) Yamazaki, H.; Ohta, K.; Endo, Y. *Tetrahedron Lett.* **2005**, *46*, 3119–3122.

(11) Fu, X.; Chan, H.-S.; Xie, Z. *J. Am. Chem. Soc.* **2007**, *129*, 8964–8965.

(12) Fox, M. A.; Nervi, C.; Crivello, A.; Low, P. J. *Chem. Commun.* **2007**, 2372–2374.

(13) (a) Evans, W. J.; Hawthorne, M. F. *J. Chem. Soc., Chem. Commun.* **1974**, 38–39. (b) Xie, Z.; Yan, C.; Yang, Q.; Mak, T. C. W. *Angew. Chem., Int. Ed.* **1999**, *38*, 1761–1763. (c) Xie, Z.; Chui, K.; Yang, Q.; Mak, T. C. W. *Organometallics* **1999**, *18*, 3947–3949. (d) Chui, K.; Yang, Q.; Mak, T. C. W.; Lam, W. H.; Lin, Z.; Xie, Z. *J. Am. Chem. Soc.* **2000**, *122*, 5758–5764. (e) Ellis, D.; Lopez, M. E.; McIntosh, R.; Rosair, G. M.; Welch, A. J. *Chem. Commun.* **2005**, 1917–1919.

(14) Zheng, F.; Zhang, J.; Fu, X.; Xie, Z. *Chem.—Asian J.* **2013**, *8*, 1886–1891, DOI: 10.1002/asia.201300240.

(15) Zhang, J.; Chan, H.-S.; Xie, Z. *Angew. Chem., Int. Ed.* **2008**, *47*, 9447–9449.

(16) Zhang, J.; Xie, Z. *Inorg. Chem.* **2012**, *51*, 12976–12987.

(17) Zhang, J.; Chan, H.-S.; Xie, Z. *Chem. Commun.* **2011**, *47*, 8082–8084.

(18) Li, Y.; Sneddon, L. G. *J. Am. Chem. Soc.* **2008**, *130*, 11494–11502.

(19) Paetzold, P. *Pure Appl. Chem.* **1991**, *63*, 345–350.

(20) Sheldrick, G. M. SADABS: Program for Empirical Absorption Correction of Area Detector Data; University of Göttingen: Germany, 1996.

(21) Sheldrick, G. M. SHELXTL 5.10 for Windows NT: Structure Determination Software Programs; Bruker Analytical X-ray systems, Inc.: Madison, WI, 1997.